



HAL
open science

Ethylzingerone, a Novel Compound with Antifungal Activity

Tristan Rossignol, Sadri Znaidi, Murielle Chauvel, Rebecca Wesgate, Laurence Decourty, Florence Menard-Szczebara, Sylvie Cupferman, Maria Dalko-Sciba, Rosemary Barnes, Jean-Yves Maillard, et al.

► **To cite this version:**

Tristan Rossignol, Sadri Znaidi, Murielle Chauvel, Rebecca Wesgate, Laurence Decourty, et al.. Ethylzingerone, a Novel Compound with Antifungal Activity. *Antimicrobial Agents and Chemotherapy*, 2021, 65 (4), pp.e02711-20. 10.1128/AAC.02711-20 . hal-03294712

HAL Id: hal-03294712

<https://hal.inrae.fr/hal-03294712>

Submitted on 31 May 2024

HAL is a multi-disciplinary open access archive for the deposit and dissemination of scientific research documents, whether they are published or not. The documents may come from teaching and research institutions in France or abroad, or from public or private research centers.

L'archive ouverte pluridisciplinaire **HAL**, est destinée au dépôt et à la diffusion de documents scientifiques de niveau recherche, publiés ou non, émanant des établissements d'enseignement et de recherche français ou étrangers, des laboratoires publics ou privés.

This is an Open Access document downloaded from ORCA, Cardiff University's institutional repository: <https://orca.cardiff.ac.uk/id/eprint/138348/>

This is the author's version of a work that was submitted to / accepted for publication.

Citation for final published version:

Rossignol, Tristan, Znaidi, Sadri, Chauvel, Murielle, Wesgate, Rebecca, Decourty, Laurence, Menard-Szczebara, Florence, Cupferman, Sylvie, Dalko-scisba, Maria, Barnes, Rosemary, Maillard, Jean-Yves, Saveanu, Cosmin and d'Enfert, Christophe 2021. Ethylzingerone, a novel compound with antifungal activity. *Antimicrobial Agents and Chemotherapy* 65 (4), e02711-20. 10.1128/AAC.02711-20

Publishers page: <http://dx.doi.org/10.1128/AAC.02711-20>

Please note:

Changes made as a result of publishing processes such as copy-editing, formatting and page numbers may not be reflected in this version. For the definitive version of this publication, please refer to the published source. You are advised to consult the publisher's version if you wish to cite this paper.

This version is being made available in accordance with publisher policies. See <http://orca.cf.ac.uk/policies.html> for usage policies. Copyright and moral rights for publications made available in ORCA are retained by the copyright holders.



1 **Ethylzingerone, a novel compound with antifungal activity.**

2

3 Tristan ROSSIGNOL^{1,§,#}, Sadri ZNAIDI^{1,2,#}, Murielle CHAUVEL¹, Rebecca WESTGATE³,
4 Laurence DECOURTY⁴, Florence MENARD-SZCZEBARA⁵, Sylvie CUPFERMAN^{5,*}, Maria
5 DALKO-SCISBA⁵, Rosemary BARNES⁶, Jean-Yves MAILLARD⁶, Cosmin SAVEANU⁴ and
6 Christophe d'ENFERT^{1,*}

7

8 ¹Unité Biologie et Pathogénicité Fongiques, Institut Pasteur, USC2019 INRA, Paris, 75015,
9 France.

10 ²Laboratoire de Microbiologie Moléculaire, Vaccinologie et Développement Biotechnologique,
11 Institut Pasteur de Tunis, University of Tunis El Manar, Tunis-Belvédère, 1002, Tunisia.

12 ³Cardiff School of Pharmacy and Pharmaceutical Sciences, Cardiff University, Cardiff, UK.

13 ⁴Unité Génétique des Interactions Macromoléculaires, Institut Pasteur, UMR3525 CNRS, Paris,
14 75015, France.

15 ⁵L'Oréal Research and Innovation, 93601 Aulnay sous Bois, France.

16 ⁶UHW, Cardiff University, Cardiff, UK.

17

18 [§] Present address: Micalis Institute, INRA, AgroParisTech, Université Paris-Saclay, 78350 Jouy-
19 en-Josas, France.

20

21 [#]Tristan ROSSIGNOL and Sadri ZNAIDI contributed equally to this work. Author order was
22 determined alphabetically.

23

24

25 *Corresponding authors.

26 Christophe d'ENFERT

27 Mailing address: Unité Biologie et Pathogénicité Fongiques, 25-28 rue du Docteur Roux, Institut

28 Pasteur, 75724 Paris Cedex 15, France

29 Phone: +33 (0)145683257

30 Fax: +33 (0)145688938

31 Electronic mail address: christophe.denfert@pasteur.fr.

32 Sylvie CUPFERMAN

33 Mailing address: L' OREAL R&I, Microbiology International Department, 188-200, rue Paul

34 Hochart, 94550 Chevilly Larue, France

35 Phone: +33 (0)149795000

36 Electronic mail address: sylvie.cupferman@rd.loreal.com

37

38 **Keywords:** Cosmetics, Ethylzingerone, Hydroxyethoxyphenyl butanone, HEPB, Antifungal,

39 Mechanism of action, *Candida albicans*

40 **Running title:** Antifungal activity of Ethylzingerone.

41

42 **ABSTRACT**

43 Preservatives increase the shelf life of cosmetic products by preventing growth of contaminating
44 microbes, including bacteria and fungi. In recent years, the Scientific Committee on Consumer
45 Safety (SCCS) has recommended the ban or restricted use of a number of preservatives due to
46 safety concerns. Here, we characterize the antifungal activity of Ethylzingerone
47 (Hydroxyethoxyphenyl butanone, HEPB), an SCCS-approved new preservative for use in rinse-
48 off, oral care and leave-on cosmetic products. We show that HEPB significantly inhibits growth
49 of *Candida albicans*, *Candida glabrata* and *Saccharomyces cerevisiae*, acting fungicidally
50 against *C. albicans*. Using transcript profiling experiments, we found that the *C. albicans*
51 transcriptome responded to HEPB exposure by increasing the expression of genes involved in
52 amino acid biosynthesis, while activating pathways involved in chemical detoxification/oxidative
53 stress response. Comparative analyses revealed that *C. albicans* phenotypic and transcriptomic
54 responses to HEPB treatment were distinguishable from those of two widely used preservatives,
55 triclosan and methylparaben. Chemogenomic analyses, using a barcoded *S. cerevisiae* non-
56 essential mutant library, revealed that HEPB antifungal activity strongly interfered with the
57 biosynthesis of aromatic amino acids. The *trp1Δ* mutants in *S. cerevisiae* and *C. albicans* were
58 particularly sensitive to HEPB treatment, a phenotype rescued by exogenous addition of
59 tryptophan to the growth medium, providing a direct link between HEPB mode-of-action and
60 tryptophan availability. Collectively, our study sheds light on the antifungal activity of HEPB, a
61 new molecule with safe properties for use as a preservative in cosmetics industry, and
62 exemplifies the powerful use of functional genomics to illuminate the mode-of-action of
63 antimicrobial agents.

64

65

66 INTRODUCTION

67 Preservatives are molecules of natural or synthetic origin intended to inhibit the
68 development of microorganisms that can contaminate food, pharmaceutical or cosmetic products
69 (1-3). Many cosmetic, household and pharmaceutical products available on the market are
70 supplemented with a variety of preservatives, including parabens (*e.g.* methylparaben, MPB),
71 isothiazolinones, organic acids, formaldehyde releasers, triclosan (TCS), and chlorhexidine (2,
72 4). Importantly, parabens appear to be the most frequently used preservatives, found in 44% of
73 cosmetics and 9% of detergents (4), while TCS reaches an estimated ~75% of the U.S.
74 population likely due to exposure *via* consumer goods and personal care products (5). Both MPB
75 and TCS are members of the phenols/alcohols chemical class of preservatives and have distinct
76 mechanisms of antimicrobial action. TCS blocks lipid biosynthesis in bacteria by specifically
77 inhibiting the enzyme enoyl-acyl carrier protein reductase (6, 7), whereas MPB exerts its
78 inhibitory activity on membrane transport and mitochondrial function; and is more active against
79 fungi than bacteria (8).

80 Although chemical preservatives prevent microbial growth, their safety is questioned by a
81 growing number of consumers and investigational reports. For instance, the Scientific
82 Committee on Consumer Safety (SCCS, European Commission) has recommended the ban or
83 restriction of using some parabens due to their potential in promoting cancerogenesis through
84 endocrine disruption (2). Yet, the scientific community considers parabens as one of the least
85 allergenic preservatives available (9) that also have an excellent safety record (10). However,
86 TCS has been recommended to be removed from all human hygiene biocidal products by the

87 SCCS, as it promotes the emergence of antimicrobial resistance and was shown to cause various
88 adverse effects in cellular and animal models of exposure to TCS (5).

89 In this context, effort from the cosmetic industry is ongoing for the identification of novel
90 preservative molecules with improved safety profile, while retaining antimicrobial activity.
91 Ethylzingerone (Hydroxyethoxyphenyl butanone, HEPB) is one of the recently investigated
92 molecules for use as a cosmetic preservative (11, 12). HEPB is a derivative of zingerone, one of
93 the active compounds in ginger and member of methoxyphenol family, known to have potent
94 pleiotropic pharmacological activities (13), including antimicrobial activity (14). Importantly, the
95 use of HEPB in rinse-off, oral care and leave-on cosmetic products was recently considered as
96 safe by the SCCS, provided it is supplied at a maximum concentration of 0.7% (wt/vol) (11, 12).

97 Fungi are responsible for a variety of infections of the skin and mucosa. Fungal growth in
98 cosmetic products can be a source of superficial infections, following a long exposure to the
99 contaminated product in day-to-day use (15). Consequently, microbial stability of cosmetic
100 products is a crucial parameter in evaluating product quality and safety, and requires the use of
101 preservatives that are well-tolerated and whose mechanism-of-action is well characterized. Many
102 approaches allowing to investigate the mode-of-action of preservatives with antifungal activity
103 rely on testing the physiological response of fungal species to preservative exposure (16). With
104 the development of fungal genetics resources and functional genomics technologies, it is possible
105 to better characterize the antifungal mode-of-action of compounds by exploring the
106 transcriptional response of fungal species to chemical treatment and screening yeast mutant
107 libraries for altered growth following chemical exposure (17). Using such approaches, we
108 characterized the antifungal activity of HEPB and provided clues on its mechanism-of-action.

109

110

111 RESULTS

112 **Characterization of HEPB antifungal activity.** We tested the antifungal activity of
113 HEPB and compared it to those of two widely used preservatives, MPB and TCS (Figure 1A).
114 We performed minimum inhibitory concentration assays and reported MIC values allowing
115 inhibition of 90% of growth (MIC_{90%}) of *C. albicans* SC5314, *C. glabrata* CBS138 and *S.*
116 *cerevisiae* BY4741 strains (Table 1). These *Candida* species are clinically relevant, both in terms
117 of prevalence (two most isolated species in candidiasis) and their ability to cause cutaneous
118 candidiasis/skin infections (18, 19), while *S. cerevisiae* is the prototypical fungal species for
119 molecular genetics analyses. MICs were evaluated in both synthetic (SD, RPMI) and rich (YPD)
120 media at 30°C (Table 1). We repeated the MIC assays with strains *C. albicans* ATCC10231, *C.*
121 *glabrata* BG2 and *S. cerevisiae* BY4742 and the results were similar between strains of the same
122 species (data not shown). MICs for MPB and HEPB were in the range of 5-20 mg/ml for all
123 tested species, except *S. cerevisiae* which shows significantly lower MIC for MPB in YPD
124 medium (1.25 mg/ml). MICs for TCS were significantly lower in all tested species, ranging from
125 0.015 to 0.25 mg/ml (Table 1).

126 To determine whether these compounds exert fungicidal or fungistatic activities, we
127 performed killing curves in rich media (YPD) by exposing *C. albicans* cells to each of the three
128 compounds at various concentrations during 0, 10, 30 and 60 min (Figure 1B). Cells were
129 washed and plated on YPD for CFU counting. At MIC_{90%}, TCS was highly fungicidal, with a
130 killing ability observed within a 10-min exposure period (Figure 1B). Compound HEPB was also
131 fungicidal, although with a lower killing ability (Figure 1B). Increasing HEPB concentration
132 (from 1×MIC to 2×MIC, Figure 1B) correlated with increased fungicidal action, resulting in the

133 viability of only ~10% of total cells after 60-min exposure. In contrast, at MIC_{90%}, MPB
134 displayed fungistatic activity and 100% of total cells were viable, even following a 60-min
135 exposure (Figure 1B).

136 Taken together, our results show that all tested compounds display antifungal activities
137 against *C. albicans*, *C. glabrata* and *S. cerevisiae*, with HEPB and TCS exerting fungicidal
138 activities, and MPB displaying a fungistatic action.

139 **Transcriptional response of *C. albicans* exposed to HEPB.** To gain insight into potential
140 molecular pathways involved in HEPB antifungal activity, we performed transcriptomics
141 analyses of *C. albicans* cells exposed to low (4 mg/ml, equivalent to 0.4×MIC) and higher (10
142 mg/ml, equivalent to 1.0×MIC) concentrations of HEPB relative to untreated cells, during 10, 30
143 and 60 min (See Materials and Methods). These treatments strongly impacted on the *C. albicans*
144 transcriptome and led to a potent modulation of gene expression (Table S1). Following treatment
145 with 4 mg/ml HEPB, we found 322, 386 and 489 upregulated and 338, 446 and 393
146 downregulated genes at time points 10, 30 and 60 min, respectively (Figure 2A, Table S1, fold-
147 change ≥ 2 or ≤ -2 , $P < 0.05$). Upon increasing the concentration of HEPB to 10 mg/ml, 754, 1052
148 and 858 genes were upregulated and 817, 1117 and 1094 genes were downregulated at time
149 points 10, 30 and 60 min, respectively (Figure 2A, Table S1). Many targets of transcription
150 factor Tac1p (20) were strongly upregulated at all tested time points (Figure 2A, blue asterisks,
151 Table S1), suggesting that HEPB treatment elicited an early and strong detoxification response
152 through activation of the expression of efflux pumps. Similarly, many genes involved in amino
153 acid biosynthesis were upregulated, including *ARG1*, *ARG3*, *ARG4*, *ARG8*, *LEU1*, others (Figure
154 2A, red asterisks, Table S1). To group the total expressed genes into clusters based on similar
155 expression patterns, we performed K-means analysis (See Materials and Methods). We generated

156 10 different clusters of co-regulated genes, among which two were selected for further analysis
157 (Figure 2B). Cluster #1 includes a subset of upregulated genes whose expression further
158 increased with increasing HEPB concentration (Figure 2B, upper panel), whereas cluster #2 may
159 reflect genes whose upregulation is required only during early events following HEPB exposure
160 (Figure 2B, lower panel). Cluster #1 was significantly enriched in genes involved in amino acid
161 biosynthesis as well as those involved in response to oxidative stress, the latter being particularly
162 observed upon exposure to 1.0×MIC (Figure 2C, upper panel). Consistently, a significant
163 proportion of the upregulated genes were targets of transcription factor Cap1p including *CIP1*,
164 *EBP1*, *OYE32*, *OYE23*, *GRP2*, *CAP1*, *TRX1*, others (Table S1) (21), suggesting that at higher
165 concentration levels, HEPB induces an oxidative stress response via Cap1p. Cluster #2 is
166 enriched in genes involved in biosynthesis of purine-containing compounds, the metabolism of
167 serine family/glycine amino acids and aromatic compound biosynthetic process (Figure 2C,
168 lower panel). It is likely that early HEPB treatment readily perturbs amino acid/purine
169 metabolism, which are interconnected processes (22). Noteworthy, we observed a sequential
170 enrichment of amino acid biosynthesis-, translation-, protein turnover- and ubiquitination-related
171 GO terms among HEPB (1.0×MIC)-upregulated genes over treatment time. These included
172 “cellular amino acid biosynthetic process” (*ARG*, *HIS*, *ILV*, *LEU*, *SER* and *TRP* genes, $P =$
173 4.53×10^{-16}) after 10-min treatment, followed by “peptide biosynthetic process” ($P = 7.39 \times 10^{-6}$),
174 “translation” ($P = 1.09 \times 10^{-5}$) and “response to starvation” ($P = 4.94 \times 10^{-4}$) after 30-min
175 treatment, then “proteolysis involved in cellular protein catabolic process” ($P = 3.06 \times 10^{-24}$),
176 “proteasome assembly” ($P = 2.17 \times 10^{-9}$) and “ubiquitin-dependent protein catabolic process” (P
177 $= 1.83 \times 10^{-22}$) after 60-min treatment.

178 To independently validate our data, *C. albicans* cells were re-grown in the presence of
179 HEPB at 1.0×MIC for 0, 10, 30 and 60 min, followed by total RNA extraction, reverse
180 transcription and qPCR analysis (Figure S1, see Materials and Methods). We tested the
181 expression of *ARG1*, *LEU1* together with *GCN4*, encoding a key regulator of amino acid
182 biosynthesis (23), at time points 10, 30 and 60 min relative to time point 0 min using *ACT1* as an
183 endogenous control (Figure S1, see Materials and Methods). The three genes were upregulated at
184 all three time points, with *ARG1* and *GCN4* displaying a gradual increase in their expression
185 levels over time (Figure S1).

186 We suggest that HEPB exposure impairs the integrity of amino acid/protein metabolism in
187 *C. albicans*, possibly through alteration of amino acid biosynthesis with a consequence on
188 protein synthesis/folding.

189 ***C. albicans* antimicrobial susceptibility is not altered upon exposure to HEPB.**

190 Because HEPB treatment transcriptionally induced a Tac1p-mediated multidrug resistance
191 response (Figure 2A), we sought to determine whether such transcriptional induction can
192 translate into acquisition of antifungal resistance in *C. albicans*. We hypothesized that induction
193 of the Tac1p-mediated multidrug resistance pathway may be a transient adaptive response to
194 preservative treatment, a commonly observed detoxification mechanism when yeast cells are
195 exposed to unrelated toxic compounds (24).

196 We first tested whether HEPB treatment could favor the development of HEPB resistance
197 in *C. albicans*, using a predictive protocol that allows to evaluate the propensity of
198 microorganisms to develop resistance to antimicrobials (See Materials and Methods). We found
199 that 24-h exposure to HEPB (0.1% wt/vol) did not alter the susceptibility of *C. albicans* strain
200 ATCC10231 to HEPB (Table 2). Next, we exposed strain ATCC10231 to HEPB under the same

201 growth conditions and determined its susceptibility to a panel of 9 antifungal agents (Table 2).
202 While a 2-fold increase in 5-Flucytosine MIC was detected (Table 2), *C. albicans*' susceptibility
203 to the remaining major antifungal agents (including azoles) was unaffected, indicating that
204 although a Tac1p-mediated transcriptional response was induced by HEPB, no significant
205 alterations in antifungal drug susceptibility were subsequently observed.

206 **Comparative transcriptomic analyses.** To determine the extent of specificity of *C.*
207 *albicans* transcriptional response to HEPB exposure as compared to those that could be induced
208 by treatment with unrelated chemical preservatives, we equivalently exposed strain SC5314 to
209 MPB (2 mg/ml, 0.4×MIC and 5 mg/ml, 1.0×MIC) and TCS (0.006 mg/ml, 0.1×MIC and 0.062
210 mg/ml, 1.0×MIC) during 10, 30 and 60 min (see Materials and Methods). We analyzed the
211 resulting transcript profiling data using hierarchical clustering. As shown in Figure 3, the
212 transcriptomes of HEPB-treated cells were clearly distinct from those of cells treated with MPB
213 and TCS, except for the transcriptomes of cells treated at low doses of MPB during 30 and 60
214 min (Figure 3), which cluster with those of 1.0×MIC HEPB-exposed cells at time points 30 and
215 60 min. Such a similarity could be explained, at least in part, by the common induction of strong
216 Tac1p- and Cap1p-mediated transcriptional signatures following HEPB and MPB treatments
217 (Table S1). This indicates that although HEPB (fungicidal) and MPB (fungistatic) seem to exert
218 different antifungal activities on *C. albicans* (Figure 1B) - consistent with distinct modes of
219 action - they may share some common effects on the *C. albicans* transcriptome. Taken together,
220 comparative analysis of the transcriptomes of *C. albicans* cells exposed to HEPB, MPB and TCS
221 suggests distinct mechanisms of antifungal activities of the three compounds, supported by little
222 overlap between their transcriptional signatures.

223 **Large-scale phenotypic profiling in *S. cerevisiae* links HEPB mode-of-action to**
224 **tryptophan availability.** We performed phenotypic profiling of all non-essential gene deletion
225 strains of the haploid *S. cerevisiae* mutant collection (25) in rich medium supplemented with
226 HEPB (see Materials and Methods). We hypothesized that our screen would identify a set of
227 genes whose individual deletion sensitizes cells to HEPB treatment, thus providing information
228 on the metabolic or cellular pathways that are most important in tolerating the toxic activity of
229 HEPB. The pool of mutants was grown for 11 generations in the absence or presence of 0.937
230 mg/ml or 1.25 mg/ml HEPB and the relative abundance for each mutant was quantified using
231 barcode microarrays (see Materials and Methods). Strikingly, the *trp1* Δ strain was the most
232 sensitive mutant among all 4,885 competing *S. cerevisiae* strains, followed by strains deleted for
233 *SOD1*, *GCN4*, *ERG2* and *DAL81* (Figure 4A, Table S2). The abundance of additional strains
234 carrying deletions in genes involved in aromatic amino acid biosynthesis (*ARO7*, *ARO3*) was
235 also decreased following HEPB treatment (Figure 4A, Table S2). We hypothesized that HEPB
236 exerts its inhibitory activity by directly or indirectly blocking pathways involved in tryptophan
237 cellular availability and tested whether tryptophan addition to HEPB-containing growth medium
238 rescues the defective growth of the *trp1* Δ mutant (Figure 4B). As shown in Figure 4B,
239 tryptophan supplementation restored the generation time of HEPB-treated *trp1* Δ mutant to levels
240 similar to those observed in the wild-type strain, contrasting with the non-addition of tryptophan
241 (Figure 4B, compare “-“ white vs. gray bars to “+” white vs. gray bars). We also confirmed the
242 specific requirement of exogenous tryptophan for restoring significant growth levels of the *trp1* Δ
243 mutant in the presence of HEPB; unlike the addition of tyrosine, phenylalanine or leucine
244 (Figure 4C, purple curve).

245 **Chemical genetic interaction profile of HEPB displays little overlap with that of TCS**
246 **and MPB.** To evaluate the extent at which the *trp1* Δ mutant phenotype is specific to HEPB
247 growth inhibitory activity, we also performed fitness profiling of the whole set of *S. cerevisiae*
248 mutant collection in the presence of TCS (15 and 20 μ g/ml) and MPB (300 and 400 μ g/ml, Table
249 S2). We found that none of these two unrelated preservatives strongly affected the growth of the
250 *trp1* Δ mutant (Figure 5, bottom row). Similarly, growth of the *gcn4* Δ , *cin8* Δ , and *sac1* Δ mutants
251 was not significantly altered by TCS or MPB treatments (Figure 5). However, the *dal81* Δ and
252 *aro7* Δ mutants were sensitive to MPB, suggesting a link between the mode-of-action of MPB
253 and amino-acid metabolism. On the other hand, sensitivity of the *sod1* Δ and *sod2* Δ mutants to
254 HEPB and MPB is likely to be linked to induction of oxidative stress by both chemicals, clearly
255 reflected in our transcript profiling data where activation of Cap1p-mediated pathway was
256 observed (Figure 2).

257 Taken together, our fitness profiling experiments in *S. cerevisiae* show that HEPB
258 interferes specifically with aromatic amino acid availability, rendering cells that cannot
259 synthesize tryptophan hypersensitive to its growth inhibitory activity.

260 ***C. albicans trp1* Δ /*trp1* Δ and *gcn4* Δ /*gcn4* Δ mutants are sensitive to HEPB treatment.**
261 Our finding that deletion of *TRP1* enhances the susceptibility of *S. cerevisiae* to HEPB treatment,
262 compared to the parental BY4742 wild-type strain (Figure 4B), fostered us to test whether a *C.*
263 *albicans trp1* Δ /*trp1* Δ mutant displays a similar phenotype under the same growth conditions. We
264 therefore exposed both *C. albicans trp1* Δ /*trp1* Δ and parental *TRP1*/*TRP1* strains to 5 mg/ml
265 HEPB in YPD medium and measured their generation time in the presence or absence of HEPB
266 (Figure 6A). In the absence of HEPB, both *trp1* Δ /*trp1* Δ and parental *TRP1*/*TRP1* strains
267 displayed similar growth rate (Figure 6A, YPD). Exposure to HEPB increased generation time of

268 the *TRP1/TRP1* strain, and further increased that of the *trp1Δ/trp1Δ* mutant (Figure 6A, + 5
269 mg/ml HEPB), phenocopying the *S. cerevisiae trp1Δ* mutant (Figure 4B).

270 Another *S. cerevisiae* mutant whose growth was significantly altered by HEPB treatment is
271 the *gcn4Δ* strain (Figure 4A). *GCN4* encodes a key transcription factor that controls the amino
272 acid biosynthesis pathway in *S. cerevisiae* and *C. albicans* (23, 26). We hypothesized that a *C.*
273 *albicans gcn4Δ/gcn4Δ* mutant would be susceptible to HEPB treatment. We tested growth of
274 both *gcn4Δ/gcn4Δ* mutant and parental *GCN4/GCN4* strain, together with the SC5314 strain by
275 spot assay on YPD medium in the presence or absence of HEPB (Figure 6B). In the absence of
276 HEPB, the three strains displayed similar growth pattern, albeit with a slight advantage for
277 SC5314 (Figure 6B, left panel). Addition of 12.5 mg/ml of HEPB significantly altered growth of
278 the *C. albicans gcn4Δ/gcn4Δ* mutant, compared to that of strains DAY286 (parental) and
279 SC5314.

280 Taken together, our results indicate that, like in *S. cerevisiae*, HEPB treatment interferes
281 with amino acid biosynthesis in *C. albicans*.

282

283
284
285
286
287
288
289
290
291
292
293
294
295
296
297
298
299
300
301
302
303
304
305

DISCUSSION

We used complementary functional genomics approaches to propose a potential mechanism-of-action of a new preservative candidate with antifungal activity, HEPB. Genome-wide expression analyses provide insights into gene function or pathways and circuits activated upon applying environmental perturbations. When a chemical stress is exerted on cells, it induces transcriptional changes reflecting both general and specific responses of the organism to alteration of one or more biological pathways that are affected by treatment with the chemical. In our case, HEPB treatment led to a transcriptional signature reflective of a potent detoxification response controlled by the multidrug resistance regulator Tac1 (Figure 2, Table S1), which we propose as a general response to chemical treatment. This response does not translate into the acquisition of stable HEPB or antifungal resistance phenotypes (Table 2), reinforcing the notion that the Tac1 response pathway is a transient adaptation mechanism to the toxicity of HEPB. However, HEPB treatment generated an early, sustained and more specific transcriptional response, reflected in the upregulation of many genes involved in amino acid biosynthesis (Figure 2, Table S1), suggesting that alteration of amino acid biosynthesis and/or availability is one of the mechanisms that could explain HEPB growth-inhibitory activity. Such transcriptional signatures can originate from the specific inhibition of the direct target of HEPB or could be part of a response that is tightly linked to the mode-of-action of HEPB. Based on previous investigations on the mode-of-action of antifungals, one could expect that inhibition of the function of a target would lead to increased expression of the genes that function in a common pathway with the target, as a result of a compensatory transcriptional response due to reduced activity of the target (27-30). Our K means analyses are in agreement with such expectations, as

306 we clearly detect the enrichment of functional categories pertaining to amino acid biosynthesis
307 and/or availability among genes that are upregulated - both early and late - following exposure to
308 HEPB (Figure 2B and 2C). A series of transcriptional profiles from cells treated with unrelated
309 compounds - in our case TCS and MPB (Figure 3) - further delineated the extent of specificity of
310 the *C. albicans* transcriptional response to HEPB treatment, and allowed to discriminate - to
311 some extent - the specific responses from the general ones, narrowing down the list of pathways
312 that could be involved in HEPB's mechanism-of-action.

313 Our transcriptional analyses could have been compared to a set of transcript profiling data
314 of *C. albicans* gene deletion or gene overexpression strains, allowing to establish and refine
315 chemical-gene associations and improve the inference of HEPB's mode-of-action. One nice
316 example reflecting this approach is the study by Hughes *et al.*, in which gene expression profiles
317 of yeast cells treated with both known and unknown drugs were compared with a compendium
318 of transcript profiles from an array of yeast deletion mutants (31). The study particularly
319 identified the mode-of-action of dyclonine, a topical anaesthetic with antimicrobial properties
320 (31). In our case, we directly focused on phenotypes rather than transcriptional signatures and
321 used chemogenomic analyses of the *S. cerevisiae* haploid knock-out collection (Figure 4), since
322 an equivalent collection in *C. albicans* is not yet available to the scientific community. Our
323 genetic approach is still powerful, since it allows to map, on the non-essential genome scale,
324 genes whose loss-of-function chemically interacts with HEPB. It also focuses on genes whose
325 deletion strongly sensitizes cells to HEPB treatment, providing a complementary strategy to
326 transcript profiling for the characterization of the mode-of-action of HEPB (32). Unlike the
327 heterozygous *S. cerevisiae* deletion, which carries individual deletions of both essential and non-
328 essential genes, our assay does not allow to identify the direct target of HEPB, which might be

329 expected to have an essential role. However, it is relevant for the identification of subsets of
330 genes and pathways that modulate HEPB sensitivity (*i.e.* displaying buffering interactions),
331 required for growth in the presence of the chemical (32). It also can mimic a double-deletion
332 mutant context, whereby one gene is deleted and the function of the second is altered through
333 chemical inhibition by HEPB. We could have used the *C. albicans* GRACE (gene replacement
334 and conditional expression) collection (33), however it relies on tetracycline derivatives to turn
335 off gene expression, which may chemically interfere with HEPB. In the event that HEPB does
336 not directly target a protein, our phenotypic assay can still identify protein-encoding genes that
337 are involved in the synthesis, import/trafficking or metabolism of HEPB target(s). Clearly,
338 complementary approaches to transcriptomics and chemogenomics are needed for the precise
339 identification of the direct target(s) of HEPB.

340 One of the mechanisms that could potentially explain the requirement of tryptophan to
341 rescue the severe growth defect of the *S. cerevisiae trp1Δ* mutant in the presence of HEPB may
342 involve direct inhibition of one of the enzymes involved in tryptophan biosynthesis or alteration
343 of the function of proteins involved in tryptophan transport into the cell. Our data argue in favor
344 of a decrease in the pool of amino acids following HEPB treatment, as we detected the
345 upregulation of many genes involved in amino acid biosynthesis as well as the activation of the
346 amino acid starvation regulator *GCN4* in our transcript profiling data (Figures S1 and 2, Table
347 S1) (26). Furthermore, the *gcn4Δ* strain was among the most depleted mutants following
348 treatment with HEPB (Figure 4A), reflecting the need for an efficient response to amino acid
349 starvation in HEPB-treated cells. In addition to *trp1Δ*, *gcn4Δ*, *aro7Δ*, *aro3Δ* and *gly1Δ* (Figure
350 4A), the list of *S. cerevisiae* mutants that are sensitive to HEPB included strains with deletions in
351 *PRS3*, involved in the synthesis of phosphoribosyl pyrophosphate (PRPP, required for

352 nucleotide, histidine and tryptophan biosynthesis) (34), *TATI*, encoding a low-affinity
353 transporter for histidine and tryptophan (35) and *TKL1*, coding for a transketolase required for
354 the synthesis of erythrose-4-phosphate, a precursor of the aromatic amino acids (36) (Table S2,
355 Figure 7). The biosynthetic processes of the aromatic amino acids tryptophan, tyrosine and
356 phenylalanine are linked together by the shikimate pathway (37) (Figure 7).
357 Phosphoenolpyruvate and erythrose 4-phosphate, deriving from glycolysis and the pentose
358 phosphate pathway, enter into a series of reactions involving the activity of the Aro1-4 enzymes,
359 whose final product is chorismate, the common precursor for the synthesis of the other two main
360 metabolites, prephenate (via Aro7) and anthranilate (via Trp2 and Trp3, Figure 7). The first
361 (prephenate) generates tyrosine and phenylalanine, the last (anthranilate) produces tryptophan
362 following a sequence of enzymatic reactions involving Trp4 (requires PRPP), Trp1, Trp3 and
363 Trp5 (37) (Figure 7). Almost all HEPB sensitive mutants with a role in amino acid metabolism
364 are deficient in key enzymes of the aromatic amino acid biosynthetic pathway described above
365 (*trp1Δ*, *aro7Δ*, *aro3Δ*, *prs3Δ* and *tkl1Δ*, Figure 7), further reinforcing our hypothesis that HEPB
366 exerts a potent perturbation of aromatic amino acid homeostasis and that tryptophan availability
367 plays a key role in HEPB growth inhibitory effect.

368 Our comparative analyses indicate that HEPB's mode-of-action is quite distinct from those
369 of two commonly used preservatives, MPB and TCS (Figures 1, 3-5). Still, our transcript
370 profiling experiments detected partial overlapping responses in *C. albicans* cells exposed to
371 HEPB and MPB (Figure 3). Both chemicals elicited Tac1- and Cap1-mediated transcriptional
372 signatures and induced the expression of a subset of genes involved in amino acid biosynthesis
373 (Table S1). We also observed some correlations between the chemogenomic profiles of HEPB-
374 and MPB-treated cells (Figure 5, Table S2), yet these two chemicals which respectively have

375 fungicidal and fungistatic activities on *C. albicans* (Figure 1B), have distinct modes of action.
376 Few studies have addressed the mechanisms through which MPB and TCS exert their antifungal
377 activities. MPB was shown to perturb microbial membrane function (8) and its effect on
378 microbial membranes was recently tested in two-dimensional lipid systems, called the Langmuir
379 monolayers (38), mimicking *Staphylococcus aureus*, *Pseudomonas aeruginosa* and *C. albicans*
380 membranes. Although MPB was shown to be more active against fungi than bacteria, the
381 strongest destructive effect of MPB was observed on bacterial membranes (38), suggesting that
382 MPB may act differently on *C. albicans*. Our transcriptomic analyses in *C. albicans* pointed to
383 perturbation of carbohydrate metabolism and activation of filamentous growth following MPB
384 treatment, whereas chemogenomics data did not clearly identify cellular processes that were
385 significantly affected by MPB. Unexpectedly, TCS treatment sensitized yeast mutants linked to
386 mitochondrial function (Table S2). In line with an alteration of mitochondrial activity, our
387 transcriptomics data revealed that many genes involved in oxidation/reduction processes were
388 upregulated upon TCS treatment (Table S1). It is possible that respiration is a major factor that
389 allows cells to survive in the presence of TCS. The potential molecular basis of this phenomenon
390 is not known, however, TCS was shown to inhibit FabI, an enoyl-acyl carrier protein reductase
391 important for the synthesis of fatty acids in bacteria (7). Eukaryotes have two different fatty acid
392 synthesis systems, one of which is mitochondrial, similar to the bacterial system and essential for
393 respiration (39). Our results together with the previous knowledge on the mechanism of action of
394 TCS in *E. coli* (6, 7) may indicate that, in yeast, the preservative affects mitochondrial fatty acid
395 synthesis leading to respiratory failure.

396

397

398 MATERIALS AND METHODS

399 **Strains, media and chemicals.** *C. albicans* strains SC5314 (40), ATCC10231 (41), CAI4
400 and CAI4t (*trp1Δ/trp1Δ*) (42), DAY286 and CJN913 (*gcn4Δ/gcn4Δ*) (43), *Candida glabrata*
401 strains BG2 (44) and CBS138 (45) and *S. cerevisiae* strains BY4741 and BY4742 (46) were used
402 in this study. Strains were routinely grown at 30°C in YPD medium (1% yeast extract, 2%
403 peptone, 2% glucose), or SD minimal medium (0.67% yeast nitrogen base without amino acids
404 (Difco), 2% glucose) supplemented with 2% agar in case of growth on a solid medium. RPMI
405 1640 (Gibco, supplemented with 2% glucose, buffered with 0.165 M morpholinepropanesulfonic
406 acid and adjusted to pH 7 with NaOH) or SD (buffered with 0.165 M MOPS and adjusted to pH
407 7 with NaOH) media were used for MIC_{90%} determinations. Stock solutions of Ethylzingerone
408 (HEPB, 0.5 g/ml), Triclosan (TCS, 1.0 g/ml) and Methylparaben (MPB, 1.0 g/ml), all provided
409 by L'Oréal, France, were prepared in dimethyl sulfoxide (or in ethanol, for fitness profiling
410 experiments in *S. cerevisiae*).

411 **Evaluation of the antifungal activities of HEPB, TCS and MPB.** Minimum inhibitory
412 concentration assays were determined in flat-bottom microtiter plates according to the EUCAST
413 method (47) with an inoculum of 1×10^5 cells/ml using strains *C. albicans* SC5314 and
414 ATCC10231, *C. glabrata* BG2 and CBS138 and *S. cerevisiae* BY4741 and BY4742. MIC_{90%}
415 were determined in triplicate at 30°C in YPD, SD pH 5.4 and RPMI pH 7.0 as well as in RPMI
416 pH 7.0 at 37°C. To determine killing curves of MPB, TCS and HEPB, an overnight culture of *C.*
417 *albicans* strain SC5314 was diluted to an optical density at 600 nm (OD₆₀₀) of 0.05 and grown to
418 an OD₆₀₀ of 0.4 in YPD and the culture was treated with various concentrations of each
419 compound or with an equal volume of solvent. Cells were sampled after 0, 10, 30 and 60 min of
420 exposure, washed, diluted 10^5 times, and plated on preservative-free YPD plates for colony-

421 forming unit (CFU) counting. Killing curves were performed in duplicate. CFUs at time 0 were
422 normalized to 100% and CFUs of other time points were calculated relative to CFUs obtained at
423 time 0.

424 **Microarray experiments.** Gene expression analyses of the *C. albicans* laboratory strain
425 SC5314 were performed by comparing planktonic cells with and without exposure to HEPB (0.4
426 \times and 1.0 \times MIC_{90%}), TCS (0.1 \times and 1.0 \times MIC_{90%}) or MPB (0.4 \times and 1.0 \times MIC_{90%}). For each
427 compound and concentration, an exponentially-grown *C. albicans* culture in YPD medium at
428 30°C was exposed to the compound and samples were collected after 10, 30 and 60 min for
429 transcript profiling. Total RNA was isolated using the RNeasy minikit (Qiagen, Courtaboeuf,
430 France) according to the manufacturer's instructions. The concentration, purity, and integrity of
431 the isolated RNA were evaluated using a Nanodrop spectrophotometer (Thermo Fisher, Illkirch,
432 France) and an Agilent 2100 Bioanalyzer (Agilent Technologies, Waldbronn, Germany). We
433 used the microarray technology at the time the project was initiated and RNA samples were
434 obtained (2010). cDNA synthesis, labelling and hybridization on *C. albicans* microarrays
435 (Agilent 026869) were performed as described in Zeidler *et al.*(48). Sample comparisons at 10,
436 30 and 60 min were performed using at least two biological replicates, and each biological
437 replicate was subjected to technical replication with dye swaps.

438 **Microarray data analysis.** Microarray scans were generated using a GenePix 4000A
439 scanner and data were acquired using the GenePix 5 software. Data analysis was carried out
440 using Arraypipe (49) and Genesis version 1.8.1(50). Data were normalized using the Loess
441 method and statistical analyses were conducted using Welch's *t*-tests. We used the August 2017
442 annotation from the *Candida* Genome Database (CGD) (51) and converted the orf19
443 nomenclature from Assembly 19 to the new Assembly 22 nomenclature (Table S1). Some

444 oligonucleotides on the microarrays (Assembly 19) did not match any ORF in the current version
445 of CGD (Assembly 22), as some genes have been removed from CGD or their coordinates
446 modified. Data for these oligonucleotides were not analysed further. The genes whose mRNA
447 level changed by at least 2-fold with $P < 0.05$ were considered significantly modulated.
448 Microarray data have been deposited at ArrayExpress under accession number E-MTAB-7908.
449 Normalized data are available in Table S1. Gene ontology analyses were performed using the
450 GO term finder tool available at the *Candida* Genome Database, with p-values calculated as
451 described in Boyle *et al.* (52) and enrichment scores were calculated as the negative values of the
452 \log_{10} -transformed p-values (p-value cut-off used was 0.05). K-means (10 clusters, 50 iterations
453 and 5 runs with 20 randomizations for testing variable dependence) and Hierarchical (Average
454 linkage WPGMA) clustering were performed using the Genesis software (50).

455 **Confirmation of transcriptomics data by RT-qPCR analysis.** Strain SC5314 was grown
456 three times independently to an OD_{600nm} of 0.8 in YPD medium at 30°C, before being exposed to
457 10 mg/ml of HEPB (1.0×MIC) for 10, 30 and 60 min. Twenty OD units were withdrawn at each
458 time point for RNA extraction (for time point 0 min, samples were withdrawn prior to addition
459 of HEPB to the growth medium). Total RNA was extracted using the RNeasy Mini Kit (Qiagen)
460 according to the manufacturer instructions. cDNA was synthesized from 1 µg of total RNA using
461 the QuantiTect Reverse Transcription Kit (Qiagen). The qPCR reactions (20 µl) were made of 5
462 µl of cDNA (25 ng) combined with 1 µl of primer mix at 10 pmol/µl each (forward and reverse
463 primers of the selected genes), 10 µL of 2X SsoAdvanced universal SYBR Green supermix (Bio-
464 Rad) and 4 µL of H₂O. Reactions were processed in a Hard-Shell 96-well PCR plate (Bio-Rad)
465 using a CFX96 real-time PCR instrument (Bio-Rad) with 1 cycle at 50°C for 2 min, 1 cycle at
466 95°C for 10 min and 40 cycles at 95°C for 15 sec and 59°C for 1 min, followed by melting-curve

467 generation to rule out amplification of unspecific products. Levels of relative gene expression (n-
468 fold) for the HEPB-treated samples at time points 10, 30 and 60 min compared to time point 0
469 min of *ARG1* (forward primer 5'-GTGAAGTTAGAGCCATCAGAGATCAA-3' and reverse
470 primer 5'-TGAACGAACGTATTCTCCTTCTGG-3') (53), *GCN4* (forward primer 5'-
471 CCAGAAATGCAAAAGGCTTC-3' and reverse primer 5'-GACTTTGGCTCCGTCATAA-3')
472 (54) and *LEU1* (forward primer 5'-GCTCCAAAGGGACAAGAATGGG-3' and reverse primer
473 5'-GTTGCTGGGTCTGGGACACT-3') (55) were calculated using the $2^{-\Delta\Delta C_T}$ method
474 (amplification of *ACT1* serving as an endogenous control gene with forward primer 5'-
475 TATGAAAGTTAAGATTATTGCTCCACCAGAAA-3' and reverse primer 5'-
476 GGAAAGTAGACAATGAAGCCAAGATAGAAC-3') (56), as follows: $\Delta C_T = C_T(\text{selected}$
477 $\text{gene}) - C_T(\text{ACT1 reference gene})$, calculated for each treatment time point, and $\Delta\Delta C_T =$
478 $\Delta C_T(\text{HEPB-treated samples}) - \Delta C_T(\text{time point 0 min sample})$. Assays were performed using 3
479 biological replicates. A two-tailed Student's *t*-test was applied by comparing, for a given gene,
480 the n-fold relative gene-expression values between treatment time points (10, 30 and 60 min,
481 Figure S1). Statistical significance threshold was $P < 0.05$.

482 **Antifungal susceptibility testing following exposure to HEPB.** This protocol was
483 previously validated to evaluate antimicrobial susceptibility profile before and after exposure to
484 an antimicrobial in 'during use' conditions (57-59). Briefly, a test suspension of $\sim 10^7$ *C. albicans*
485 ATCC10231 cells was prepared in 1 ml of Tryptone Sodium Chloride (TSC, 1.0 g/l tryptone, 8.5
486 g/l NaCl) medium. This suspension (1 ml) was added to 9 ml of HEPB (diluted in H₂O) at 1.25
487 times the required concentration (0.1% w/v) and incubated for 24 h at 20°C. Following exposure,
488 *C. albicans* cells were filtered through a 0.2 µm filter and washed with 5 ml neutralizer (1.5%
489 v/v Tween 80 and 3% w/v lecithin, Fisher Scientific), then with 5 ml TSC. The filter was placed

490 in a bottle with 5 ml TSC and 5 g of glass beads, then vortexed for 1 min to recover survivors.
491 Antifungal susceptibility testing was performed 3 times independently, using the colorimetric
492 microdilution assay Sensititre YeastOne w/Micafungin & Anidulafungin (YO10) system
493 (ThermoFisher Scientific, UK) as per manufacturer's recommendation. MIC values were
494 determined for anidulafungin, amphotericin B, micafungin, caspofungin, 5-flucytosine,
495 posaconazole, voriconazole, itraconazole and fluconazole (Table 2). Susceptibility to HEPB was
496 tested by determining MIC before and after 0.1% HEPB (w/v) exposure using the BS EN ISO:
497 20776-1 (2006) microdilution protocol. The highest HEPB concentration tested of 2% w/v
498 corresponded to ~ 3× the prospective in-use concentration in formulae. The MIC was taken as
499 the lowest concentration of HEPB that showed no growth after 24 h incubation at 25°C.

500 **Fitness assay with a barcoded haploid *S. cerevisiae* knock-out collection.** Fitness assays
501 were performed with 4,885 *S. cerevisiae* haploid deletion mutants from the systematic deletion
502 collection as described in Giaever *et al.* (Background strain BY4741) (25). Mutants were grown
503 individually in 96 deep-well plates at 30°C for 2 days in YPD medium, pooled and aliquots were
504 stored at -80°C. We did an initial growth test for *S. cerevisiae* in YPD medium at 30°C with 5
505 different concentrations of TCS, MPB and HEPB, all solubilized in pure ethanol as stock
506 solutions. Final concentrations used for the fitness assay were: HEPB, 3.4 mM (700 mg/l); MPB,
507 1.95 mM (300 mg/l) and TCS, 51 µM (15 mg/l). The pool of mutants was grown for 11
508 generations in the absence or presence of each preservative and growth of individual strains in
509 the different cultures was determined by amplifying, labelling and hybridizing the barcodes on
510 custom barcode microarrays (Agilent G2509F - AMADID N°026035) as described in detail in
511 Malabat & Saveanu (60). Briefly, genomic DNA from the collected cells was extracted with
512 phenol-chloroform by extensive vortexing in the presence of glass beads (425-600 nm size).

513 Primers U1 and KU (Table S3) were used to amplify the upstream barcodes and primers KD and
514 D1 (Table S3) to amplify the downstream barcodes. 25 cycles of PCR with an annealing
515 temperature of 50°C were used. The resulting PCR products were verified by electrophoresis on
516 an agarose gel and used in a labeling PCR reaction with the Cy3 or Cy5 5'-labelled
517 oligonucleotides U2comp (Table S3) for the upstream tags and D2comp (Table S3) for the
518 downstream tags and unlabelled U1 and D1 as a control. Only 15 cycles of amplification were
519 used in the labelling step. The labelled PCR products were mixed and precipitated in the
520 presence of linear acrylamide and of a mixture of complementary oligonucleotides (U1, D1,
521 U2block, D2block, Table S3) in four-fold molar excess to avoid binding of the fluorescently
522 labelled oligonucleotides to the microarray probes. Hybridization was performed using the DIG
523 Easy Hyb buffer (Roche Applied Science), at 24°C, overnight, in a rotating Agilent hybridization
524 chamber. The slides were washed in decreasing concentrations of SSPE buffer (10 mM
525 potassium phosphate (pH 7.4), 150 mM NaCl, 0.5 mM EDTA, 0.05% (w/v) Triton X100) down
526 to 0.2 x SSPE, dried and treated immediately with the Agilent Stabilization and Drying Solution
527 to avoid ozone-induced degradation of the Cy5 fluorophore. Scanning was performed on a
528 Genepix 4200AL scanner and the images were analysed using Axon Genepix Pro 7. We filtered
529 the data according to our previous estimates of the reliability of the microarray signal. Filtered
530 data were normalized using the Loess algorithm (R package *marray*, Bioconductor) (61)
531 separately for signals coming from upstream or downstream barcodes. The average of the values
532 for the upstream barcode and the downstream barcode was calculated. The \log_2 of the ratio
533 between the signal obtained for a given mutant growing with and without preservative was used
534 as an estimate of the drug's effect on the growth rate of the mutant. Data processing and
535 statistical analyses were performed using R package (<http://cran.r-project.org/>). Complete dataset

536 of the fitness profiling data was deposited at Gene Expression Omnibus database under accession
537 # GSE125353.

538 **Spot and liquid growth assays.** Fitness assay data were validated using individually
539 grown *S. cerevisiae* or *C. albicans* mutants in 96-well plates. Cells were grown three times
540 independently with agitation in a Tecan Sunrise plate reader at 30°C in YPD medium and optical
541 densities at 600 nm were recorded every 5 to 10 min, followed by growth curve generation and
542 calculation of doubling times as described previously (62). The *S. cerevisiae* (parental BY4742
543 and the *trp1*Δ mutant derivative) and *C. albicans* (parental CAI4 and the *trp1*Δ/*trp1*Δ mutant
544 derivative CAI4t (42), kindly provided by Dr. Bernard Turcotte) strains were cultured in the
545 absence or presence of 2 mg/ml and 5 mg/ml HEPB, respectively. Amino acids were added to
546 the *S. cerevisiae* cultures at a final concentration of 2 mM. For spot assays, *C. albicans* strains
547 DAY286, the *gcn4*Δ/*gcn4*Δ mutant derivative (43) and SC5314 were resuspended in water to an
548 OD_{600nm} of 0.1. Tenfold serial dilutions of each strain were spotted onto YPD plates
549 supplemented with 12.5 mg/ml of HEPB. The plates were incubated for 3 days at 30°C.

550

551

552 **ACKNOWLEDGMENTS**

553 The Authors would like to thank Drs. Bernard TURCOTTE and Aaron MITCHELL for kindly
554 providing the *C. albicans trp1Δ/trp1Δ* and *gcn4Δ/gcn4Δ* mutants. We are indebted to Charlotte
555 TACHEAU for technical help in omics analyses, Patricio GUERREIRO for funding assistance,
556 Isabelle CASTIEL for scientific publication assistance, Gabriel Ahmad KHODR for draft
557 reviewing, Émilie BIERQUE for excellent technical assistance and Alain JACQUIER for helpful
558 discussions.

559

560 **FUNDING**

561 This work has been supported by grants from L'Oréal (to CD, CS and JYM), the French
562 Government's Investissements d'Avenir program (Laboratoire d'Excellence Integrative Biology
563 of Emerging Infectious Diseases, ANR-10-LABX-62-IBEID to CD) and the Agence Nationale
564 de la Recherche (ANR-08-JCJC-0019-01/GENO-GIM to CS). SZ is an Institut Pasteur
565 International Network Affiliate Program Fellow.

566

567 **TRANSPARENCY DECLARATIONS**

568 This research was funded by L'Oréal, France. Scientists at L'Oréal, France have been involved
569 in validating the study design proposed by scientists at Institut Pasteur and Cardiff University, in
570 discussing the results obtained by scientists at Institut Pasteur and Cardiff University and in
571 commenting the manuscript prepared by scientists at Institut Pasteur and Cardiff University.

572 Scientists at L'Oréal, France are co-authors of this manuscript or acknowledged for their
573 contributions.

575 **REFERENCES**

- 576 1. Chiu CH, Huang SH, Wang HM. 2015. A Review: Hair Health, Concerns of Shampoo
577 Ingredients and Scalp Nourishing Treatments. *Curr Pharm Biotechnol* 16:1045-52.
- 578 2. Halla N, Fernandes IP, Heleno SA, Costa P, Boucherit-Otmani Z, Boucherit K,
579 Rodrigues AE, Ferreira I, Barreiro MF. 2018. Cosmetics Preservation: A Review on
580 Present Strategies. *Molecules* 23.
- 581 3. Leyva Salas M, Mounier J, Valence F, Coton M, Thierry A, Coton E. 2017. Antifungal
582 Microbial Agents for Food Biopreservation-A Review. *Microorganisms* 5.
- 583 4. Yazar K, Johnsson S, Lind ML, Boman A, Liden C. 2011. Preservatives and fragrances
584 in selected consumer-available cosmetics and detergents. *Contact Dermatitis* 64:265-72.
- 585 5. Weatherly LM, Gosse JA. 2017. Triclosan exposure, transformation, and human health
586 effects. *J Toxicol Environ Health B Crit Rev* 20:447-469.
- 587 6. Levy CW, Roujeinikova A, Sedelnikova S, Baker PJ, Stuitje AR, Slabas AR, Rice DW,
588 Rafferty JB. 1999. Molecular basis of triclosan activity. *Nature* 398:383-4.
- 589 7. McMurry LM, Oethinger M, Levy SB. 1998. Triclosan targets lipid synthesis. *Nature*
590 394:531-2.
- 591 8. Soni MG, Taylor SL, Greenberg NA, Burdock GA. 2002. Evaluation of the health
592 aspects of methyl paraben: a review of the published literature. *Food Chem Toxicol*
593 40:1335-73.
- 594 9. Fransway AF, Fransway PJ, Belsito DV, Warshaw EM, Sasseville D, Fowler JF, Jr.,
595 DeKoven JG, Pratt MD, Maibach HI, Taylor JS, Marks JG, Mathias CGT, DeLeo VA,

- 596 Zirwas JM, Zug KA, Atwater AR, Silverberg J, Reeder MJ. 2019. Parabens. *Dermatitis*
597 30:3-31.
- 598 10. Sasseville D, Alfalah M, Lacroix JP. 2015. "Parabenoia" Debunked, or "Who's Afraid of
599 Parabens?". *Dermatitis* 26:254-9.
- 600 11. Bernauer U. 2017. Opinion of the scientific committee on consumer safety (SCCS) -
601 Final version of the opinion on Ethylzingerone - 'Hydroxyethoxyphenyl Butanone'
602 (HEPB) - Cosmetics Europe No P98 - in cosmetic products. *Regul Toxicol Pharmacol*
603 88:330-331.
- 604 12. Bernauer U. 2019. Opinion of the Scientific Committee on Consumer safety (SCCS) -
605 Opinion on Ethylzingerone - 'Hydroxyethoxyphenyl Butanone' (HEPB) - Cosmetics
606 Europe No P98 - CAS No 569646-79-3 - Submission II (eye irritation). *Regul Toxicol*
607 *Pharmacol* 107:104393.
- 608 13. Kundu JK, Na HK, Surh YJ. 2009. Ginger-derived phenolic substances with cancer
609 preventive and therapeutic potential. *Forum Nutr* 61:182-92.
- 610 14. Kumar L, Chhibber S, Kumar R, Kumar M, Harjai K. 2015. Zingerone silences quorum
611 sensing and attenuates virulence of *Pseudomonas aeruginosa*. *Fitoterapia* 102:84-95.
- 612 15. Dao H, Lakhani P, Police A, Kallakunta V, Ajjarapu SS, Wu KW, Ponkshe P, Repka
613 MA, Narasimha Murthy S. 2017. Microbial Stability of Pharmaceutical and Cosmetic
614 Products. *AAPS PharmSciTech* 19:60-78.
- 615 16. Mundy RD, Cormack B. 2009. Expression of *Candida glabrata* adhesins after exposure to
616 chemical preservatives. *J Infect Dis* 199:1891-8.
- 617 17. Znaidi S. 2015. Strategies for the Identification of the Mode-Of-Action of Antifungal
618 Drug Candidates., p 183-209. *In* Coste AT, Vendeputte P (ed), *Antifungals: From*

- 619 Genomics to Resistance and the Development of Novel Agents. Caister Academic Press,
620 Norfolk, UK.
- 621 18. Kashem SW, Kaplan DH. 2016. Skin Immunity to *Candida albicans*. *Trends Immunol*
622 37:440-450.
- 623 19. Kuhbacher A, Burger-Kentischer A, Rupp S. 2017. Interaction of *Candida* Species with
624 the Skin. *Microorganisms* 5.
- 625 20. Liu TT, Znaidi S, Barker KS, Xu L, Homayouni R, Saidane S, Morschhauser J, Nantel A,
626 Raymond M, Rogers PD. 2007. Genome-wide expression and location analyses of the
627 *Candida albicans* Tac1p regulon. *Eukaryot Cell* 6:2122-38.
- 628 21. Znaidi S, Barker KS, Weber S, Alarco AM, Liu TT, Boucher G, Rogers PD, Raymond
629 M. 2009. Identification of the *Candida albicans* Cap1p regulon. *Eukaryot Cell* 8:806-20.
- 630 22. Ljungdahl PO, Daignan-Fornier B. 2012. Regulation of amino acid, nucleotide, and
631 phosphate metabolism in *Saccharomyces cerevisiae*. *Genetics* 190:885-929.
- 632 23. Tripathi G, Wiltshire C, Macaskill S, Tournu H, Budge S, Brown AJ. 2002. Gcn4 co-
633 ordinates morphogenetic and metabolic responses to amino acid starvation in *Candida*
634 *albicans*. *EMBO J* 21:5448-56.
- 635 24. Fardeau V, Lelandais G, Oldfield A, Salin H, Lemoine S, Garcia M, Tanty V, Le Crom S,
636 Jacq C, Devaux F. 2007. The central role of PDR1 in the foundation of yeast drug
637 resistance. *Journal of Biological Chemistry* 282:5063-5074.
- 638 25. Giaever G, Chu AM, Ni L, Connelly C, Riles L, Veronneau S, Dow S, Lucau-Danila A,
639 Anderson K, Andre B, Arkin AP, Astromoff A, El-Bakkoury M, Bangham R, Benito R,
640 Brachat S, Campanaro S, Curtiss M, Davis K, Deutschbauer A, Entian KD, Flaherty P,
641 Foury F, Garfinkel DJ, Gerstein M, Gotte D, Guldener U, Hegemann JH, Hempel S,

642 Herman Z, Jaramillo DF, Kelly DE, Kelly SL, Kotter P, LaBonte D, Lamb DC, Lan N,
643 Liang H, Liao H, Liu L, Luo C, Lussier M, Mao R, Menard P, Ooi SL, Revuelta JL,
644 Roberts CJ, Rose M, Ross-Macdonald P, Scherens B, et al. 2002. Functional profiling of
645 the *Saccharomyces cerevisiae* genome. *Nature* 418:387-91.

646 26. Hinnebusch AG. 2005. Translational regulation of GCN4 and the general amino acid
647 control of yeast. *Annu Rev Microbiol* 59:407-50.

648 27. Lee RE, Liu TT, Barker KS, Rogers PD. 2005. Genome-wide expression profiling of the
649 response to ciclopirox olamine in *Candida albicans*. *J Antimicrob Chemother* 55:655-62.

650 28. Liu TT, Lee RE, Barker KS, Wei L, Homayouni R, Rogers PD. 2005. Genome-wide
651 expression profiling of the response to azole, polyene, echinocandin, and pyrimidine
652 antifungal agents in *Candida albicans*. *Antimicrob Agents Chemother* 49:2226-2236.

653 29. Niewerth M, Kunze D, Seibold M, Schaller M, Korting HC, Hube B. 2003. Ciclopirox
654 olamine treatment affects the expression pattern of *Candida albicans* genes encoding
655 virulence factors, iron metabolism proteins, and drug resistance factors. *Antimicrob
656 Agents Chemother* 47:1805-17.

657 30. te Welscher YM, van Leeuwen MR, de Kruijff B, Dijksterhuis J, Breukink E. 2012.
658 Polyene antibiotic that inhibits membrane transport proteins. *Proc Natl Acad Sci U S A*
659 109:11156-9.

660 31. Hughes TR, Marton MJ, Jones AR, Roberts CJ, Stoughton R, Armour CD, Bennett HA,
661 Coffey E, Dai H, He YD, Kidd MJ, King AM, Meyer MR, Slade D, Lum PY, Stepaniants
662 SB, Shoemaker DD, Gachotte D, Chakraburttty K, Simon J, Bard M, Friend SH. 2000.
663 Functional discovery via a compendium of expression profiles. *Cell* 102:109-26.

- 664 32. Giaever G, Nislow C. 2014. The yeast deletion collection: a decade of functional
665 genomics. *Genetics* 197:451-65.
- 666 33. Roemer T, Jiang B, Davison J, Ketela T, Veillette K, Breton A, Tandia F, Linteau A,
667 Sillaots S, Marta C, Martel N, Veronneau S, Lemieux S, Kauffman S, Becker J, Storms
668 R, Boone C, Bussey H. 2003. Large-scale essential gene identification in *Candida*
669 *albicans* and applications to antifungal drug discovery. *Molecular Microbiology* 50:167-
670 181.
- 671 34. Carter AT, Beiche F, Hove-Jensen B, Narbad A, Barker PJ, Schweizer LM, Schweizer
672 M. 1997. PRS1 is a key member of the gene family encoding
673 phosphoribosylpyrophosphate synthetase in *Saccharomyces cerevisiae*. *Mol Gen Genet*
674 254:148-56.
- 675 35. Schmidt A, Hall MN, Koller A. 1994. Two FK506 resistance-conferring genes in
676 *Saccharomyces cerevisiae*, TAT1 and TAT2, encode amino acid permeases mediating
677 tyrosine and tryptophan uptake. *Mol Cell Biol* 14:6597-606.
- 678 36. Sundstrom M, Lindqvist Y, Schneider G, Hellman U, Ronne H. 1993. Yeast TKL1 gene
679 encodes a transketolase that is required for efficient glycolysis and biosynthesis of
680 aromatic amino acids. *J Biol Chem* 268:24346-52.
- 681 37. Braus GH. 1991. Aromatic amino acid biosynthesis in the yeast *Saccharomyces*
682 *cerevisiae*: a model system for the regulation of a eukaryotic biosynthetic pathway.
683 *Microbiol Rev* 55:349-70.
- 684 38. Flasiński M, Kowal S, Broniatowski M, Wydro P. 2018. Influence of Parabens on
685 Bacteria and Fungi Cellular Membranes: Studies in Model Two-Dimensional Lipid
686 Systems. *J Phys Chem B* 122:2332-2340.

- 687 39. Hiltunen JK, Schonauer MS, Autio KJ, Mittelmeier TM, Kastaniotis AJ, Dieckmann CL.
688 2009. Mitochondrial fatty acid synthesis type II: more than just fatty acids. *J Biol Chem*
689 284:9011-5.
- 690 40. Gillum AM, Tsay EY, Kirsch DR. 1984. Isolation of the *Candida albicans* gene for
691 orotidine-5'-phosphate decarboxylase by complementation of *S. cerevisiae* *ura3* and *E.*
692 *coli* *pyrF* mutations. *Molecular & General Genetics* 198:179-182.
- 693 41. Lingappa BT, Prasad M, Lingappa Y, Hunt DF, Biemann K. 1969. Phenethyl alcohol and
694 tryptophol: autoantibiotics produced by the fungus *Candida albicans*. *Science* 163:192-4.
- 695 42. Lebel K, MacPherson S, Turcotte B. 2006. New tools for phenotypic analysis in *Candida*
696 *albicans*: the *WAR1* gene confers resistance to sorbate. *Yeast* 23:249-259.
- 697 43. Nobile CJ, Mitchell AP. 2009. Large-scale gene disruption using the *UAU1* cassette.
698 *Methods MolBiol* 499:175-194.
- 699 44. Cormack BP, Falkow S. 1999. Efficient homologous and illegitimate recombination in
700 the opportunistic yeast pathogen *Candida glabrata*. *Genetics* 151:979-87.
- 701 45. Koszul R, Malpertuy A, Frangeul L, Bouchier C, Wincker P, Thierry A, Duthoy S, Ferris
702 S, Hennequin C, Dujon B. 2003. The complete mitochondrial genome sequence of the
703 pathogenic yeast *Candida (Torulopsis) glabrata*. *FEBS Lett* 534:39-48.
- 704 46. Brachmann CB, Davies A, Cost GJ, Caputo E, Li J, Hieter P, Boeke JD. 1998. Designer
705 deletion strains derived from *Saccharomyces cerevisiae* S288C: a useful set of strains and
706 plasmids for PCR-mediated gene disruption and other applications. *Yeast* 14:115-32.
- 707 47. Cuenca-Estrella M, Arendrup MC, Chryssanthou E, Dannaoui E, Lass-Flörl C, Sandven
708 P, Velegraki A, Rodriguez-Tudela JL. 2007. Multicentre determination of quality control
709 strains and quality control ranges for antifungal susceptibility testing of yeasts and

710 filamentous fungi using the methods of the Antifungal Susceptibility Testing
711 Subcommittee of the European Committee on Antimicrobial Susceptibility Testing
712 (AFST-EUCAST). *Clin Microbiol Infect* 13:1018-22.

713 48. Zeidler U, Bougnoux ME, Lupan A, Helynck O, Doyen A, Garcia Z, Sertour N, Clavaud
714 C, Munier-Lehmann H, Saveanu C, d'Enfert C. 2013. Synergy of the antibiotic colistin
715 with echinocandin antifungals in *Candida* species. *J Antimicrob Chemother* 68:1285-96.

716 49. Hokamp K, Roche FM, Acab M, Rousseau ME, Kuo B, Goode D, Aeschliman D, Bryan
717 J, Babiuk LA, Hancock RE, Brinkman FS. 2004. ArrayPipe: a flexible processing
718 pipeline for microarray data. *Nucleic Acids Res* 32:W457-9.

719 50. Sturn A, Quackenbush J, Trajanoski Z. 2002. Genesis: cluster analysis of microarray
720 data. *Bioinformatics* 18:207-8.

721 51. Skrzypek MS, Binkley J, Binkley G, Miyasato SR, Simison M, Sherlock G. 2017. The
722 *Candida* Genome Database (CGD): incorporation of Assembly 22, systematic identifiers
723 and visualization of high throughput sequencing data. *Nucleic Acids Res* 45:D592-D596.

724 52. Boyle EI, Weng S, Gollub J, Jin H, Botstein D, Cherry JM, Sherlock G. 2004.
725 GO::TermFinder--open source software for accessing Gene Ontology information and
726 finding significantly enriched Gene Ontology terms associated with a list of genes.
727 *Bioinformatics* 20:3710-5.

728 53. Nett JE, Lepak AJ, Marchillo K, Andes DR. 2009. Time course global gene expression
729 analysis of an in vivo *Candida* biofilm. *J Infect Dis* 200:307-13.

730 54. Sundaram A, Grant CM. 2014. A single inhibitory upstream open reading frame (uORF)
731 is sufficient to regulate *Candida albicans* GCN4 translation in response to amino acid
732 starvation conditions. *RNA* 20:559-67.

- 733 55. De Cremer K, De Brucker K, Staes I, Peeters A, Van den Driessche F, Coenye T,
734 Cammue BP, Thevissen K. 2016. Stimulation of superoxide production increases
735 fungicidal action of miconazole against *Candida albicans* biofilms. *Sci Rep* 6:27463.
- 736 56. Cabral V, Znaidi S, Walker LA, Martin-Yken H, Dague E, Legrand M, Lee K, Chauvel
737 M, Firon A, Rossignol T, Richard ML, Munro CA, Bachellier-Bassi S, d'Enfert C. 2014.
738 Targeted Changes of the Cell Wall Proteome Influence *Candida albicans* Ability to Form
739 Single- and Multi-strain Biofilms. *PLoS Pathog* 10:e1004542.
- 740 57. Maillard JY, Bloomfield S, Coelho JR, Collier P, Cookson B, Fanning S, Hill A,
741 Hartemann P, McBain AJ, Oggioni M, Sattar S, Schweizer HP, Threlfall J. 2013. Does
742 microbicide use in consumer products promote antimicrobial resistance? A critical review
743 and recommendations for a cohesive approach to risk assessment. *Microb Drug Resist*
744 19:344-54.
- 745 58. Knapp L, Amezcua A, McClure P, Stewart S, Maillard JY. 2015. Development of a
746 protocol for predicting bacterial resistance to microbicides. *Appl Environ Microbiol*
747 81:2652-9.
- 748 59. Wesgate R, Grasha P, Maillard JY. 2016. Use of a predictive protocol to measure the
749 antimicrobial resistance risks associated with biocidal product usage. *Am J Infect Control*
750 44:458-64.
- 751 60. Malabat C, Saveanu C. 2016. Identification of Links Between Cellular Pathways by
752 Genetic Interaction Mapping (GIM). *Methods Mol Biol* 1361:325-43.
- 753 61. Gentleman RC, Carey VJ, Bates DM, Bolstad B, Dettling M, Dudoit S, Ellis B, Gautier
754 L, Ge Y, Gentry J, Hornik K, Hothorn T, Huber W, Iacus S, Irizarry R, Leisch F, Li C,
755 Maechler M, Rossini AJ, Sawitzki G, Smith C, Smyth G, Tierney L, Yang JY, Zhang J.

756 2004. Bioconductor: open software development for computational biology and
757 bioinformatics. *Genome Biol* 5:R80.

758 62. St Onge RP, Mani R, Oh J, Proctor M, Fung E, Davis RW, Nislow C, Roth FP, Giaever
759 G. 2007. Systematic pathway analysis using high-resolution fitness profiling of
760 combinatorial gene deletions. *Nat Genet* 39:199-206.

761

762

763 **TABLES**764 **TABLE 1.** MIC_{90%}^a (mg/ml) for Methylparaben, Triclosan and HEPB.

Species/Strain	Growth medium	MPB^b	TCS^b	HEPB^b
	YPD	5	0.06	10
<i>C. albicans</i> SC5314	RPMI	5	0.06	10
	SD	10	0.25	20
<i>C. glabrata</i> CBS138	YPD	10	0.06	20
	RPMI	5	0.12	10
	SD	10	0.12	20
<i>S. cerevisiae</i> BY4741	YPD	1.25	0.015	10

765 ^a MIC_{90%} value, determined as the first concentration (mg/ml) of the preservative able to reduce
766 growth by 90% compared with that of control cells grown in the absence of preservative in YPD,
767 RPMI at pH 7 and SD at pH 5.4.

768 ^b MPB, Methylparaben; TCS, Triclosan; HEPB, Ethylzingerone.

769

770

771 **Table 2.** Antifungal and HEPB susceptibilities of *C. albicans* ATCC10231 (MIC, $\mu\text{g/ml} \pm$
772 standard deviation) after 24-h exposure to 0.1% HEPB (w/v, n=3).

Treatment*	HEPB	AND	AB	MF	CAS	FC	PZ	VOR	IZ	FZ
-HEPB	5mg/ml ± 0.00	0.10 \pm 0.03	0.50 \pm 0.00	0.015 \pm 0.00	0.06 \pm 0.00	0.12 \pm 0.00	0.06 \pm 0.00	0.06 \pm 0.00	0.25 \pm 0.00	2.00 \pm 0.00
+HEPB	5mg/ml ± 0.00	0.10 \pm 0.03	0.50 \pm 0.03	0.015 \pm 0.00	0.06 \pm 0.00	0.25 \pm 0.00	0.06 \pm 0.00	0.06 \pm 0.00	0.25 \pm 0.00	2.00 \pm 0.00

773 *Treatment: -HEPB, no addition of HEPB; +HEPB, addition of 0.1% HEPB (wt/vol); HEPB:
774 Ethylzingerone; AND: Anidulafungin; AB: Amphotericin B; MF: Miconazole; CAS:
775 Caspofungin; FC: 5-Flucytosine; PZ: Posaconazole; VOR: Voriconazole; IZ: Itraconazole; FZ:
776 Fluconazole.

777

778

779 **FIGURE LEGENDS**

780 **FIGURE 1. Antifungal activities of Ethylzingerone, Triclosan and Methylparaben. A.**

781 Chemical structures of Methylparaben (MPB), Triclosan (TCS) and Ethylzingerone (HEPB). **B.**

782 Representative killing curves of *C. albicans* strain SC5314 exposed to different concentrations of

783 each preservative in YPD medium. *x*-axis, exposure time (min) to the indicated concentrations of

784 each preservative; *y*-axis, percentage of colony-forming unit (CFU) counts at each time point

785 relative to CFU counts at time point 0. (■) control with solvent alone, (■) MPB at 5 mg/ml

786 (1×MIC), (●) HEPB at 10 mg/ml (1×MIC), (●) HEPB at 20 mg/ml (2×MIC) and (□) TCS 0.062

787 mg/ml (1×MIC).

788

789 **FIGURE 2. Transcript profiling in *C. albicans* exposed to Ethylzingerone. A.** Heat maps of

790 the 50 highest (left panel, red) and lowest (right panel, green) transcriptionally-modulated genes

791 (Log_2 -transformed ratios are shown and color scale indicates the maximum and minimum

792 expression ratios, +/-10.08) following exposure of *C. albicans* SC5314 to 4 mg/ml (0.4×MIC) or

793 10 mg/ml (1.0×MIC) HEPB for 10, 30 and 60 min (combination of 2 to 3 biological replicates in

794 each condition). The most upregulated (descending signal intensity, sorted by average expression

795 in all conditions, left panel) or downregulated (ascending signal intensity, sorted by average

796 expression in all conditions, right panel) genes in HEPB-treated vs. untreated cells are indicated

797 with their corresponding name or systematic nomenclature on the right side of each panel. Genes

798 highlighted with a blue asterisk are those that are transcriptionally modulated by activation of

799 transcription factor Tac1p (20), while genes highlighted with a red asterisk are those involved in

800 amino acid biosynthesis. Heat maps were constructed using Genesis version 1.8.1 (50). **B.** K-

801 means profile plots of 2 selected clusters (Cluster #1, 118 genes, upper panel and cluster #2, 83

802 genes, lower panel) out of 10 clusters generated through mining of the complete transcript
803 profiling dataset (Table S1) using Genesis version 1.8.1.(50) The expression dynamics of each
804 gene (\log_2 -transformed ratios, gray line) are plotted on the y -axis, whereas the experimental
805 condition is indicated on the x -axis (bottom). **C.** GO-term enrichment scores (black bars,
806 representing the negative value of \log_{10} transformed p-values shown on the x -axis) of the
807 significantly enriched functional categories (p-value < 0.05) among the 118 and 83 genes from
808 K-means clusters #1 (upper chart) and #2 (lower chart), respectively. The GO terminologies are
809 indicated on the y -axis. The number of genes belonging to each GO terminology are indicated
810 between parentheses.

811

812 **FIGURE 3. Comparative analysis of the transcriptomics data.** Hierarchical clustering using
813 Average Linkage WPGMA (clustering of both genes and conditions) showing the relationships
814 between the distinct 18 compound treatments (Top). Each gene is represented by a rectangle
815 colored according to the level of up-regulation (red) or down-regulation (green) as indicated in
816 the colored scale showing adjusted maximal (+5.0) and minimal (-5.0) \log_2 -transformed ratios.
817 The relatedness between conditions is shown on the upper cladogram, whereas relatedness
818 between gene expression profiles are indicated on the left cladogram. The hierarchical clustering
819 heatmap was generated using Genesis version 1.8.1 (50).

820

821 **FIGURE 4. Phenotypic profiling in *S. cerevisiae* links HEPB mode-of-action to tryptophan**
822 **availability.** **A.** Histogram depicting the relative abundance of each group of *S. cerevisiae*
823 mutants (histogram bins) measured as the \log_2 -transformed ratio of barcode signal intensity in
824 HEPB-treated samples (n=3) compared to untreated control sample (x -axis). The number of

825 strains per histogram bin are shown on the y-axis. Mutants with significantly decreased
826 abundance following HEPB treatment are shown on the left part of the histogram, whereas those
827 with increased relative abundance are shown on the right part of the histogram. **B.** Parental
828 BY4742 (gray bar) and the *trp1*Δ mutant derivative (white bar) were grown in the absence (-) or
829 presence (+) of 0.4 mg/ml tryptophan in YPD medium (YPD) supplemented (+ 2 mg/ml HEPB,
830 +1 mg/ml HEPB) or not (YPD) with 2 mg/ml or 1 mg/ml HEPB. Generation times (in hours) of
831 each strain in each condition are indicated on the y-axis calculated as the mean of 3
832 independently grown cultures with error bars denoting standard deviations. **C.** Growth curves of
833 the *trp1*Δ mutant grown in YPD medium (YPD) or in YPD medium supplemented with 2 mg/ml
834 HEPB (+ 2 mg/ml HEPB) are depicted in different colors depending on the identity of the amino
835 acid being added to the growth medium. Turbidity (OD_{600nm}, y-axis) was recorded every 5 min as
836 a function of time (hours, x-axis) in a Tecan Sunrise device.

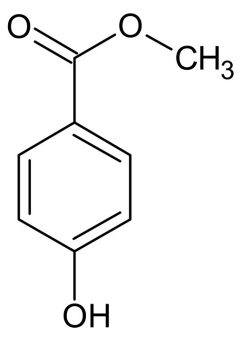
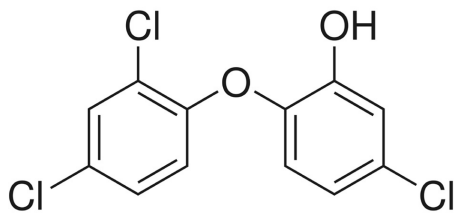
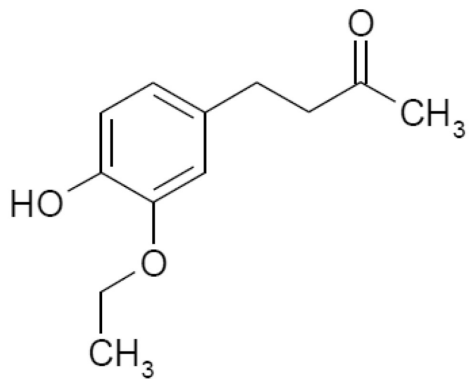
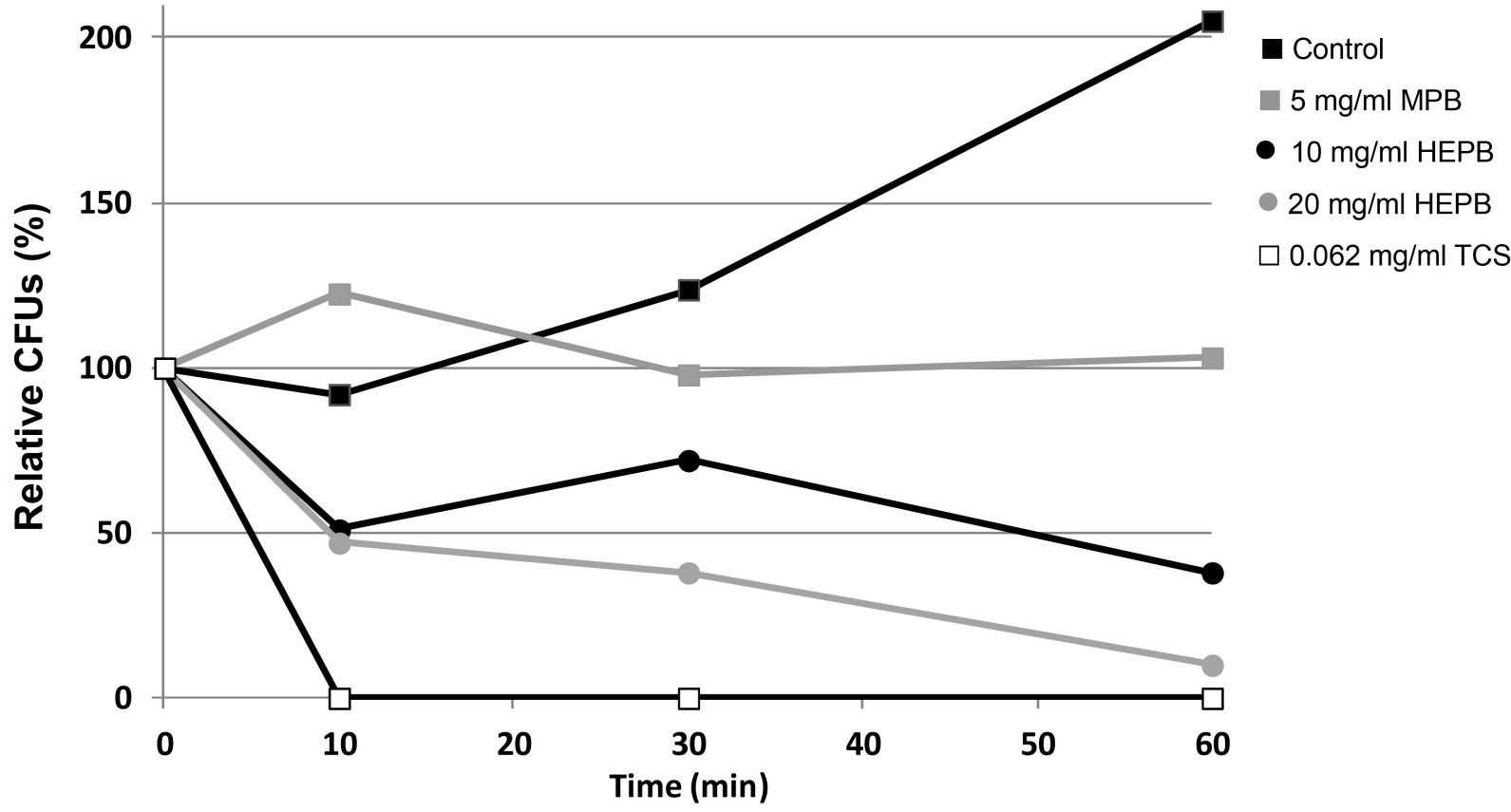
837

838 **FIGURE 5. Chemical-genetic interactions of TCS and MPB with *S. cerevisiae* mutants that**
839 **are sensitive to HEPB.** Fitness profiling matrix displaying the relative abundance of mutant
840 strains *sod2*Δ, *aro7*Δ, *vrp1*Δ, *sac1*Δ, *cin8*Δ, *dal81*Δ, *erg2*Δ, *gcn4*Δ, *sod1*Δ and *trp1*Δ following
841 exposure to TCS (15 and 20 μg/ml), MPB (300 and 400 μg/ml) and HEPB (937 and 1,250
842 μg/ml). Fitness defect intensities (numerical values) are also displayed as colored squares,
843 according to the color scale shown at the bottom of the panel. Negative values indicate decreased
844 abundance of the corresponding mutant.

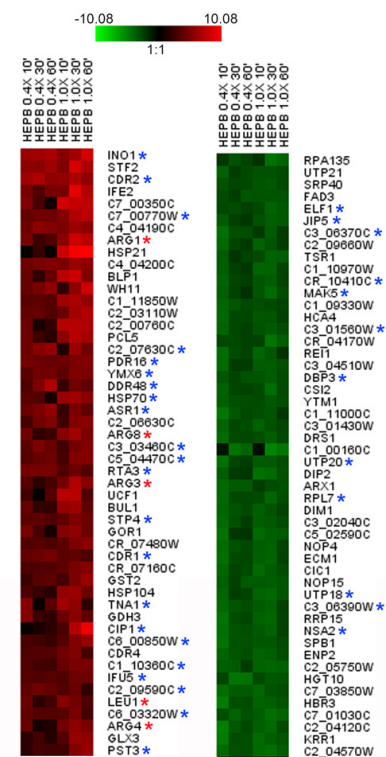
845

846 **Figure 6. *C. albicans trp1Δ/trp1Δ* and *gcn4Δ/gcn4Δ* mutants are sensitive to HEPB**
847 **treatment. A.** Parental CAI4 (*TRP1/TRP1*, gray bar) and the *trp1Δ/trp1Δ* mutant derivative
848 (white bar) were grown in YPD medium supplemented (5 mg/ml HEPB) or not (Control) with 5
849 mg/ml HEPB. Generation time (in hours) of each strain in each condition are indicated on the y-
850 axis, calculated as the mean of values from 3 independently grown cultures with error bars
851 denoting standard deviations. Asterisk, $P < 0.05$ based on a Welch's *t*-test comparing mean
852 values of the *trp1Δ/trp1Δ* mutant to those of the parental strain *TRP1/TRP1* in the presence of
853 HEPB (5 mg/ml HEPB). **B.** HEPB susceptibility of strains DAY286, *gcn4Δ/gcn4Δ* (*gcn4-/-*) and
854 SC5314 was tested by spot assay on YPD plates supplemented (or not supplemented, left panel,
855 Control) with 12.5 mg/ml of HEPB (12.5 mg/ml HEPB, right panel). Plates were incubated at
856 30°C for 3 days.

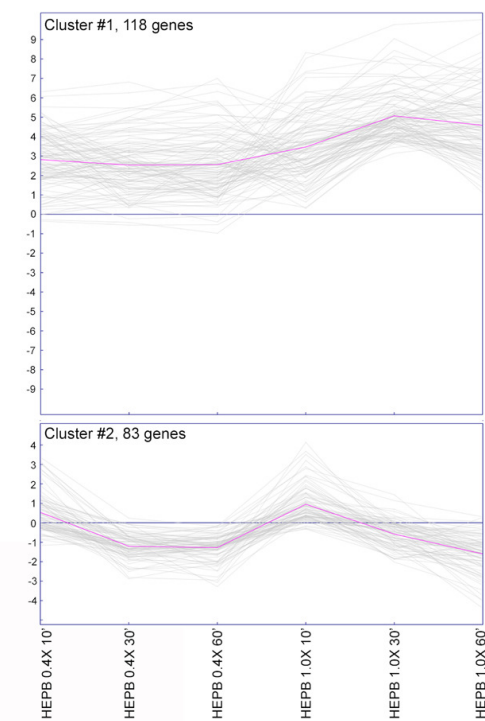
857 **FIGURE 7. Simplified schematic representation of the aromatic amino acid biosynthetic**
858 **pathway.** A sequence of enzymatic reactions encoded by many *ARO* and *TRP* genes are crucial
859 for the biosynthesis of aromatic amino acids. Specific steps from the pentose phosphate pathway
860 (top box, left) and glycolysis (top box, right) generate Erythrose-4-P and Phosphoenolpyruvate,
861 which are processed by the products of *ARO* and *TRP* genes to generate Tryptophan (whose
862 chemical structure is shown at the bottom left), Tyrosine and Phenylalanine. Tryptophan can also
863 be taken up from the medium owing to the activity of a low-affinity permease encoded by *TATI*
864 (grey oval). Genes with a role in amino acid biosynthesis whose deletion strongly sensitizes *S.*
865 *cerevisiae* to HEPB treatment are colored in red.

A**Methylparaben****Triclosan****Ethylzingerone****B**

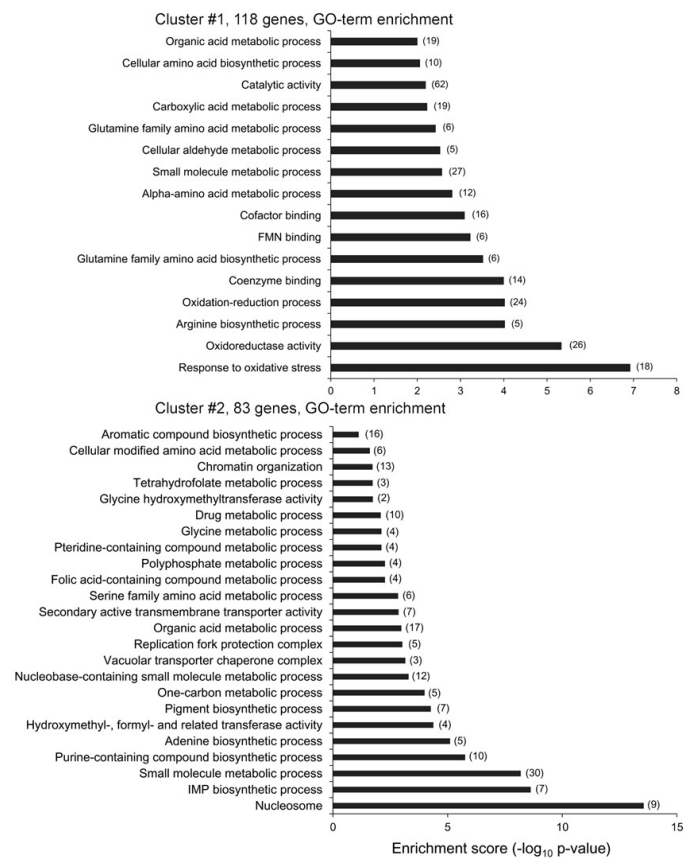
A



B



C



-5.0

1:1

5.0

HEPB 0.4X 30'

HEPB 0.4X 60'

HEPB 0.4X 10'

HEPB 1.0X 10'

HEPB 1.0X 30'

HEPB 1.0X 60'

MPB 0.4X 30'

MPB 0.4X 60'

TCS 0.1X 30'

TCS 0.1X 60'

MPB 0.4X 10'

TCS 0.1X 10'

TCS 1.0X 30'

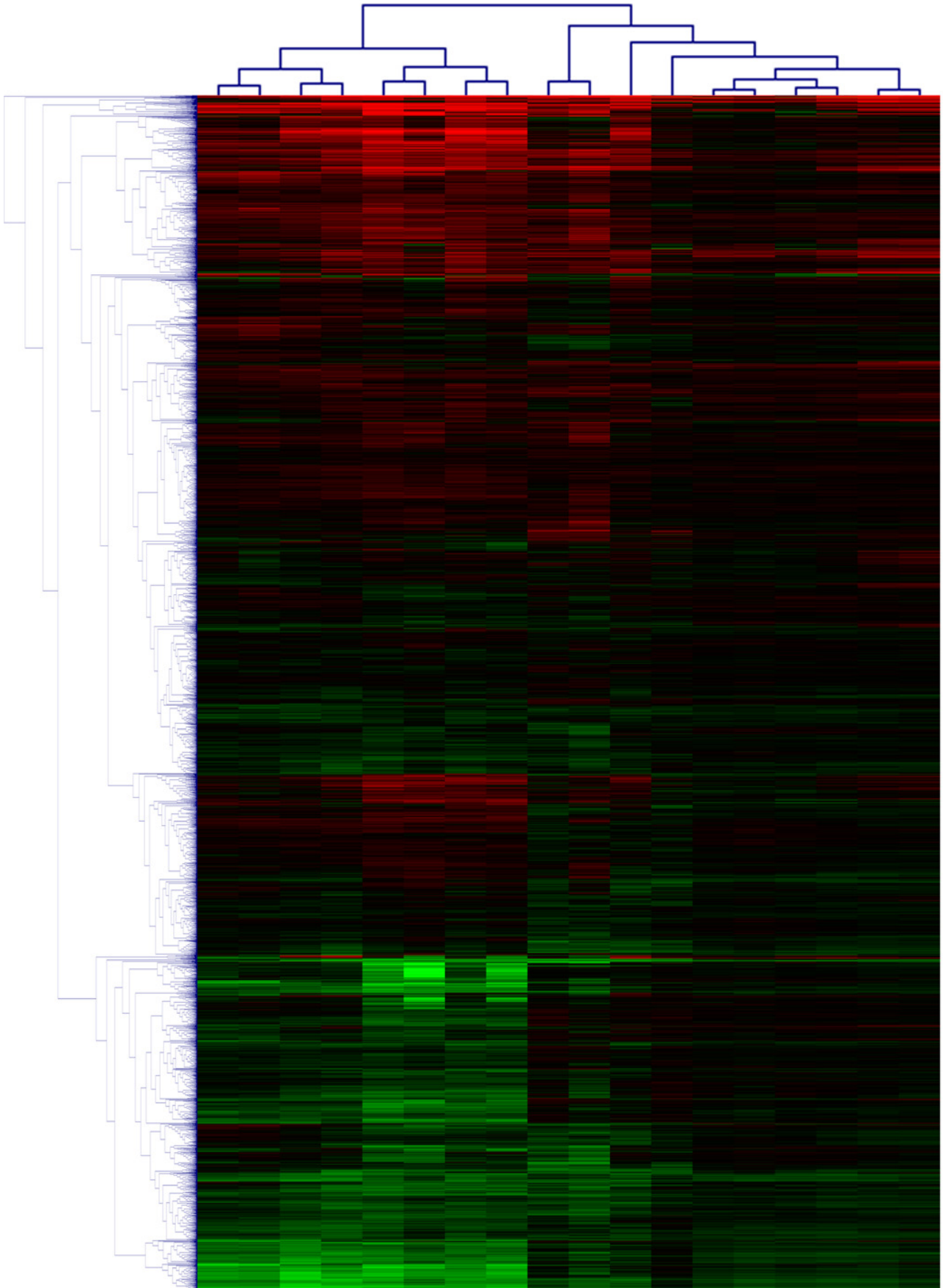
TCS 1.0X 60'

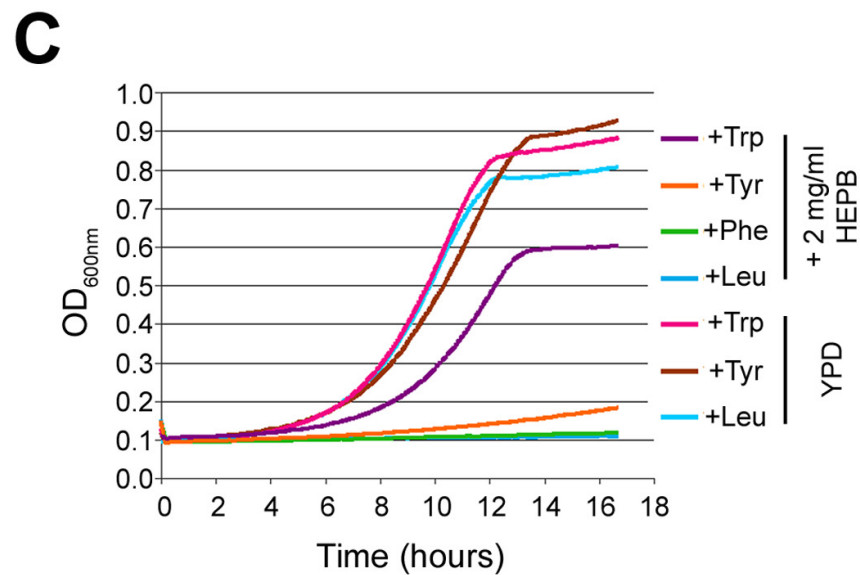
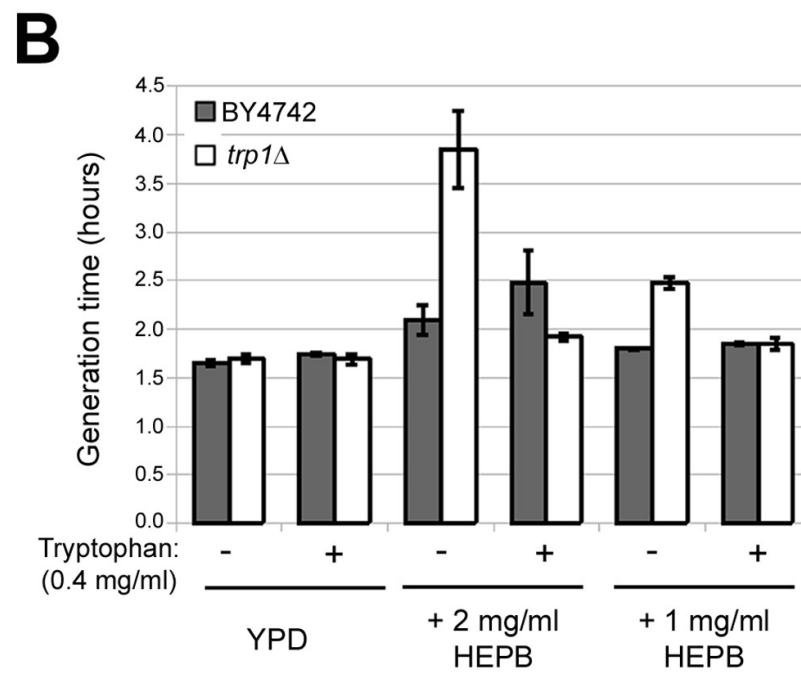
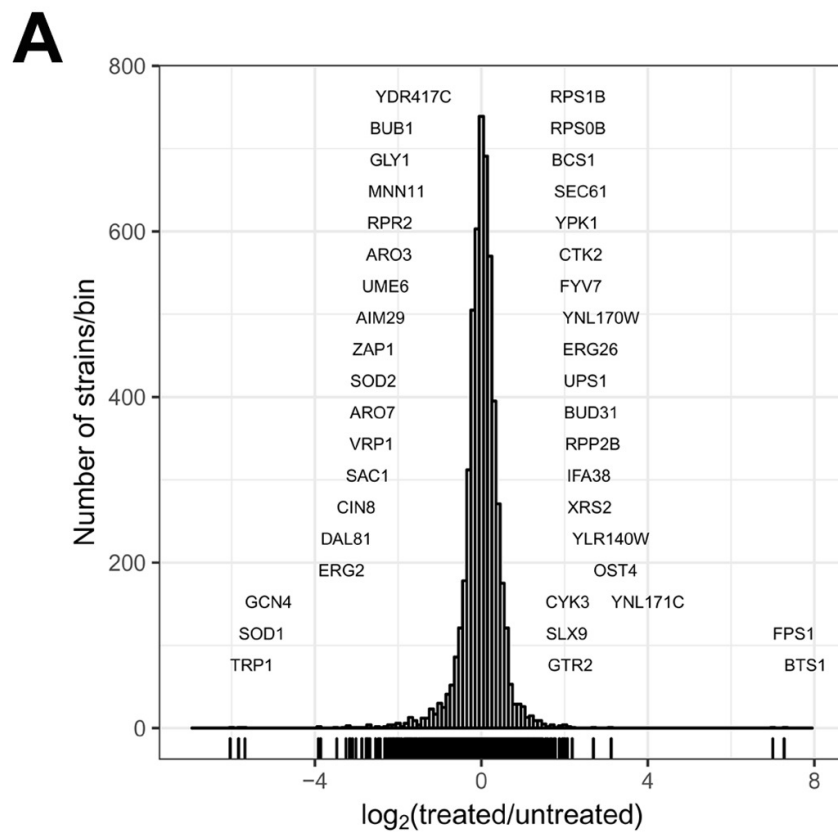
TCS 1.0X 10'

MPB 1.0X 10'

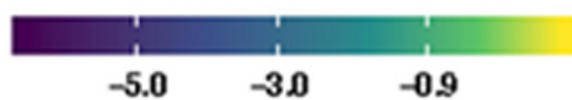
MPB 1.0X 30'

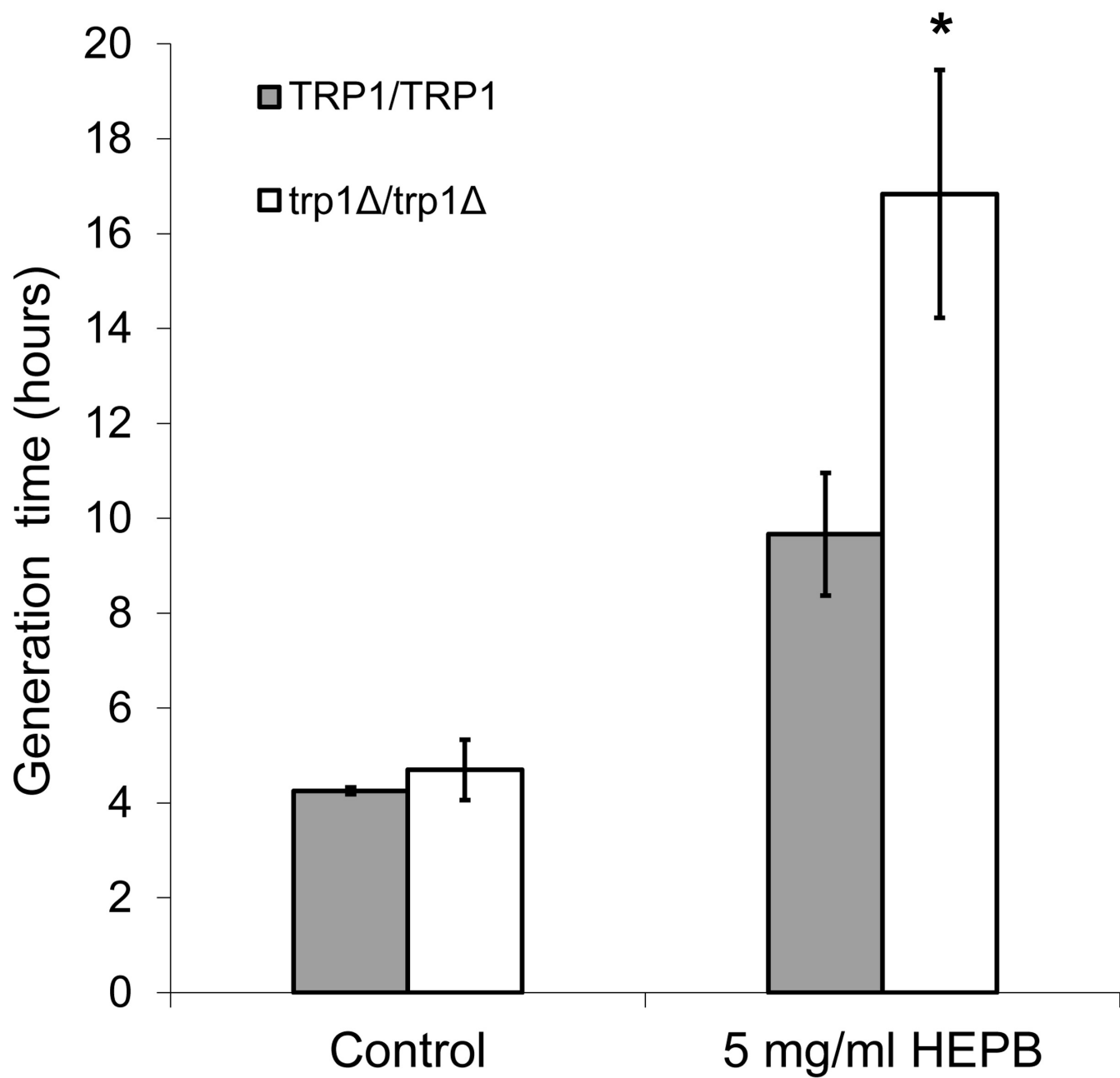
MPB 1.0X 60'





	TCS 15 $\mu\text{g/ml}$	TCS 20 $\mu\text{g/ml}$	MPB 300 $\mu\text{g/ml}$	MPB 400 $\mu\text{g/ml}$	HEPB 937 $\mu\text{g/ml}$	HEPB 1250 $\mu\text{g/ml}$
SOD2	-0.1	1	-3.6		-2.1	-4.2
ARO7	-0.7	0.2	-1.4	-3.3	-2.4	-3.9
VRP1	-2.2	-3.2	0.1	0.5	-1.6	-4.8
SAC1	-0.4	-0.1	-0.2	-1.4	-1.7	-4.8
CIN8	0.4	0.8	0	0	-3	-3.9
DAL81	-2.3	-0.1	-5.7	-6.5	-3	-4.7
ERG2	-0.3	-1.2	-5.9		-4.8	-3
GCN4	0.6	0.6	0.1	0.1	-6.3	-5.1
SOD1	-0.2	-0.4	-1.9	-2.4	-6.5	-5.1
TRP1	0.2	0.2	-0.5	-1	-5.5	-6.5



A**B**